Check for updates

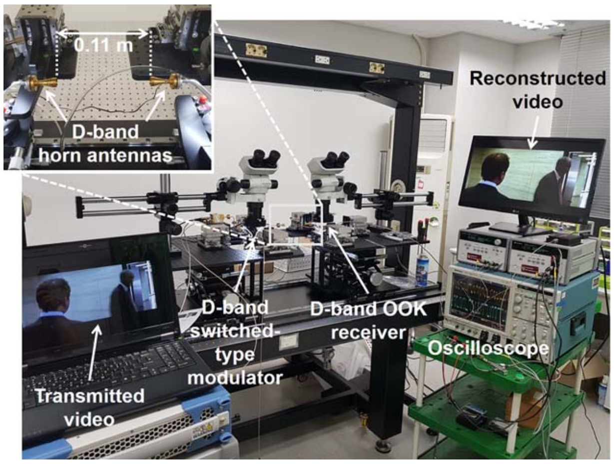

FIGURE 7 Experimental setup for HD video transfer through an air channel [Color figure can be viewed at wileyonlinelibrary.com]

To demonstrate the high-speed demodulation capability of the ED, an OOK receiver integrating the ED and an on-chip D-band amplifier is tested for an air channel, as shown in Figure 5. The simulated gain of D-band amplifier is 7 dB at 120 GHz and the 3-dB bandwidth is 11.5 GHz. A 120-GHz carrier is modulated with 2^9 PRBS by a D-band switched-type modulator. The OOK-modulated signal is transferred between two 20-dBi horn antennas apart by a distance of 0.11 m. The OOK receiver including the ED, followed by a baseband amplifier, demodulates the received signal. Figure 6 shows the measured eye-diagram of the baseband output when the data rate changes from 1 to 4 Gbps. It should be noted that the maximum data rate is limited by the narrowband on-chip D-band amplifier, not by the ED that operates over the entire D-band.

An HD video signal is also transferred through the air channel and is reconstructed by the receiver to validate the practical application of the ED. The video signal is encoded and decoded, following the SMPTE 292M standard with a data rate of 1.485 Gbps. As can be seen in Figure 7, the transmitted video signal is well reconstructed at the receiver output.

4 | CONCLUSION

A D-band ED is fabricated in a low-cost 65-nm bulk CMOS process for high-speed OOK wireless communication. The measured average responsivity and NEP are 1.16 kV/W and 234 pW/Hz$^{1/2}$, respectively, over the entire D-band. The ED effectively demodulates the OOK signal up to 4-Gbps over an air-channel distance of 0.11 m. Moreover, an HD video signal at 1.485 Gbps is successfully demodulated and reconstructed using an OOK receiver integrating this ED.

ACKNOWLEDGMENT

This work was supported by the Defensive Specialized Laboratory for Terahertz Electronic Devices through the Korea Agency for Defense Development (UD150043RD).

ORCID

Sanggeun Jeon http://orcid.org/0000-0001-7453-2331

REFERENCES

[1] Fujishima M, Motoyoshi M, Katayama K, Takano K, Ono N, Fujimoto R. 98 mW 10 Gbps wireless transceiver chipset with D-band CMOS circuits. *IEEE J Solid State Circuits.* 2013;48(10):2273–2284.

[2] Byeon CW, Yoon CH, Park CS. A 67-mW 10.7-Gb/s 60-GHz OOK CMOS transceiver for short-range wireless communications. *IEEE Trans Microwave Theory Techn.* 2013;61(9):3391–3401.

[3] Yu X, Rashtian H, Mirabbasi S, Pande PP, Heo D. An 18.7-Gb/s 60-GHz OOK demodulator in 65-nm CMOS for wireless network-on-chip. *IEEE Trans Circuits Syst I Regular Pap.* 2015;62(3):799–806.

[4] Chai S, Hong S. "Sub-THz OOK receiver for chip to chip data link," *2015 Asia-Pacific Microwave Conference (APMC)*, Nanjing, 2015:1–3.

How to cite this article: Suh B, Jeon S. A full D-band CMOS envelope detector for high-speed OOK wireless communication. *Microw Opt Technol Lett*. 2018; 60:1619–1622. https://doi.org/10.1002/mop.31212

Received: 22 November 2017

DOI: 10.1002/mop.31211

Low-cost metamaterial absorber using three-dimensional circular truncated cone

Youngseo Yoon[1] | Daecheon Lim[1] | Manos M. Tentzeris[2] | Sungjoon Lim[1]

[1] School of Electrical and Electronics Engineering, College of Engineering, Chung-Ang University, Seoul 156-756, Korea

[2] School of Electrical and Computer Engineering, Georgia Institute of Technology, Atlanta, Georgia 30332-0250

Correspondence
Manos M. Tentzeris, School of Electrical and Computer Engineering, Georgia Institute of Technology, Atlanta, GA 30332-0250.
Email: etentze@ece.gatech.edu or

Sungjoon Lim, School of Electrical and Electronics Engineering, Chung-Ang University, Seoul 156-756, Korea.
Email: sungjoon@cau.ac.kr

Y. Yoon and D. Lim equally contributed as the first author.

Abstract

In this article, we propose a low-cost three-dimensional (3D) printed metamaterial absorber. The proposed metamaterial consists of a periodic structure of circular truncated cones. The dielectric materials supporting the circular truncated cone are made from a poly(lactic acid) filament using the 3D printer. The conductor of the circular truncated cone is developed by spraying silver-coated copper. The performance of the proposed absorber is numerically and experimentally investigated. The simulated and measured absorptivity are 91% and 95% at 10.8 and 10.81 GHz, respectively. As a result of the 3D printing and silver spray coating processes, the proposed absorber can be easily fabricated at a low cost.

KEYWORDS

metamaterial absorber, three-dimensional electromagnetic absorber, three-dimensional (3D) printing technology

1 | INTRODUCTION

Metamaterials are structures that are artificially designed to possess characteristics that are not yet found in nature.[1] Metamaterials are used in various fields such as super lenses using a negative refractive index, invisibility cloaking using electromagnetic wave diffraction, miniaturization of RF parts, and stealth technology.[2,3] Particularly, an electromagnetic wave absorber using a metamaterial can obtain a high absorptivity with a thin thickness by matching its impedance with the air and removing the reflected wave.[4] Conventional electromagnetic wave absorbers can only operate at certain frequencies, or are bulky at low frequencies.[5,6] In contrast, the metamaterial absorber can be fabricated on a printed circuit board (PCB), is very thin, and can exhibit high absorptivity over a wide frequency band.[7,8]

Recently, three-dimensional (3D) printing technology has been applied to fabrication of an electrical small antenna and ultra-wide band antenna.[9,10] Currently, the fabrication of the metamaterial absorber through the PCB technology was limited to design in planar geometry. The proposed metamaterial absorber using 3D print technology can realize more efficient and diverse designs on 3D geometry than using PCB technology. In this work, we demonstrate the feasibility of 3D-printed absorber with a simple design.

For PCB fabrication, many steps have to be taken.[11] For this reason, the PCB manufacturing process is a long, complex, and expensive. Compared to PCB technology, the 3D printing technology provides benefits of short manufacturing time, low cost, simple process and no chemical waste.[12] For the 3D printing process, there are many methods of implementing conductive patterns have been introduced in recent studies, such as metal printing,[13] the use of a conductive filler,[14] hybrid additive manufacturing (AM) build sequencing,[15] and spraying conductive materials.[16–21] Of these options, the spraying method offers the advantages, such as low cost, simplicity of fabrication, and short processing time.

In this article, we propose a low-cost 3D-printed metamaterial absorber. In order to achieve simple and low-cost fabrication, we apply 3D printing technology and use a silver-coated copper conductive coating instead of using conductive ink. The unit structure of proposed metamaterial has a circular truncated cone shape pattern. The substrate and truncated con shape is realized by poly(lactic acid) (PLA) filament using the 3D printer. By spraying silver-coated copper on the circular truncated cone, the conductive pattern of the metamaterial absorber is established.

2 | ABSORBER DESIGN

Figure 1 illustrates a unit cell of the proposed absorber. The unit structure consists of a silver-coated truncated cone, a

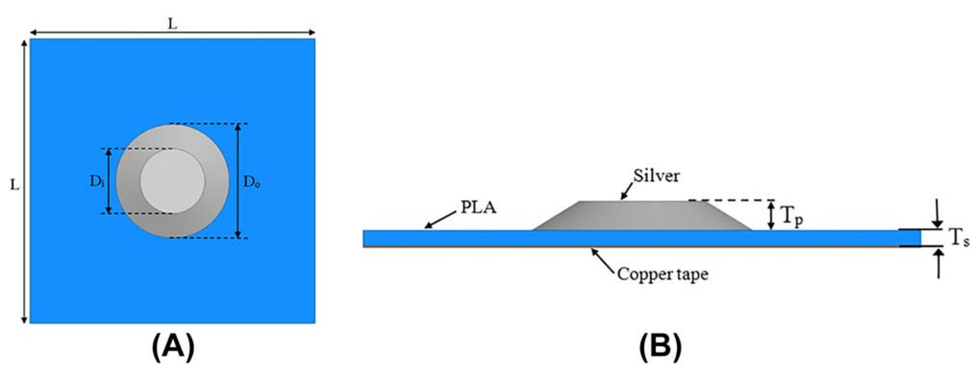

FIGURE 1 A, Top view and B, side view of the proposed unit cell: $L = 21$, Di = 4.8, Do = 8.4, Tp = 11, and Ts = 0.55 (unit: mm) [Color figure can be viewed at wileyonlinelibrary.com]

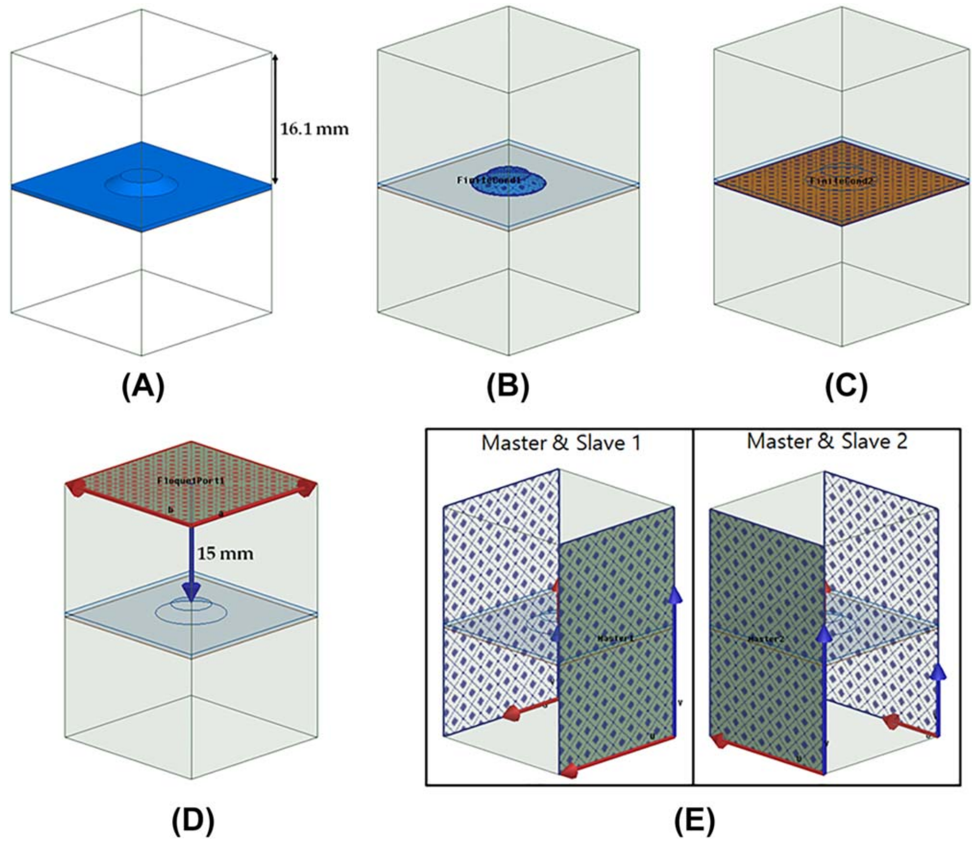

FIGURE 2 Simulation set up for the proposed metamaterial absorber: A, air box, material assignment for B, the top pattern and C, ground; D, Floquet port; and E, master/slave boundary condition [Color figure can be viewed at wileyonlinelibrary.com]

substrate made of PLA, and a copper ground plane on the bottom. The values of the parameters in Figure 1A are $L = 21$, $\mathrm{Di} = 4.8$, and $\mathrm{Do} = 8.4$ mm. Figure 1B shows the side view of the designed unit cell of the proposed absorber. We designed a truncated cone with a height of $\mathrm{Tp} = 11$ mm and used a PLA substrate with a thickness of $\mathrm{Ts} = 0.55$ mm. A 0.6 mm thick copper tape is used for the bottom ground.

In order to simulation of the proposed absorber, we used a finite-element method (FEM)-based ANSYS high-frequency structure simulator and all material parameters for EM simulation are characterized from the measurement results. The surface resistance of the silver-coated conductor is 0.04 ohms/square. Because the PLA dielectric material is dispersive and isotropic, its dielectric constant and loss

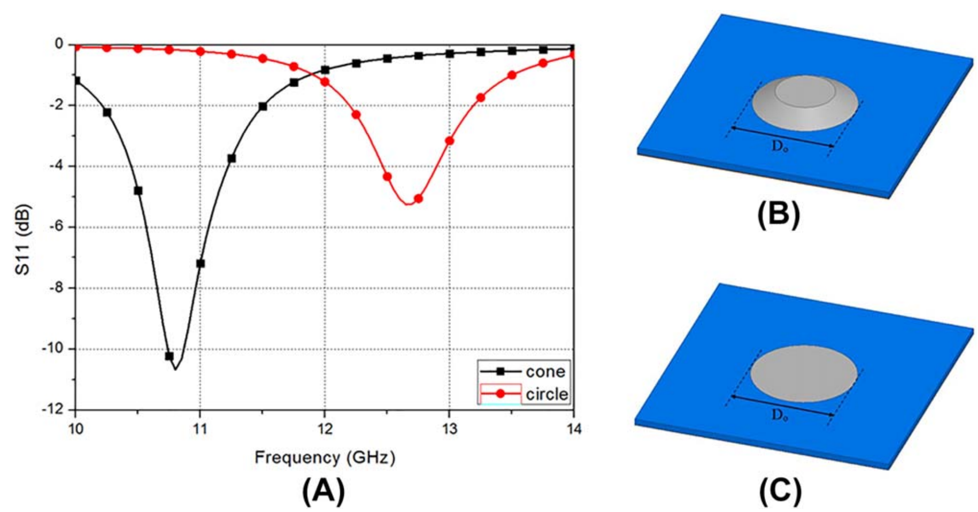

FIGURE 3 A, Simulated S11 of the proposed 3D circular truncated cone and 2D circular patch. B, Geometry of the proposed 3D circular truncated cone. C, Geometry of the 3D circular patch [Color figure can be viewed at wileyonlinelibrary.com]

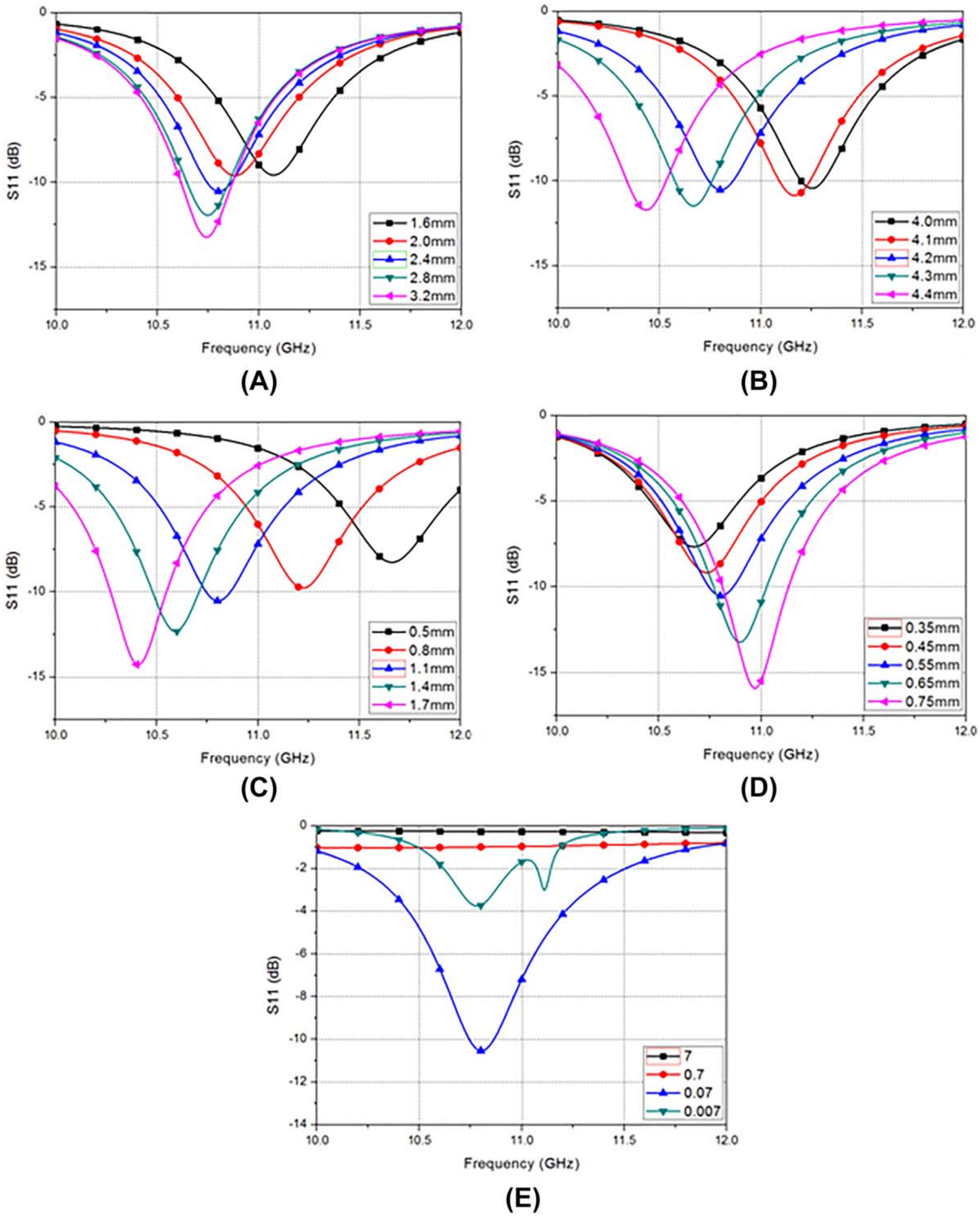

FIGURE 4 Simulated return losses of the proposed metamaterial absorber for different values of A, Di; B, Do; C, Tp; D, Ts; and E, loss tangent of the PLA substrate [Color figure can be viewed at wileyonlinelibrary.com]

tangent are characterized from the waveguide measurement. At 10 GHz, the extracted dielectric constant and loss tangent of the PLA are 2.09 and 0.07, respectively. We designed the unit cell after considering the minimum 3D printing resolution which is 200 μm. The EM simulation setup for infinite periodic structure is illustrated in Figure 2. First of all, the air box of larger than half-wavelength size is drawn in order to satisfy the far field condition as illustrated in Figure 2A. The material of the top pattern is assigned as the surface impedance with 0.04 ohms/square as shown in Figure 2B. The bottom ground is assigned as the copper material as shown in Figure 2C. In order to excite the EM wave, the Floquet port is used in order to realize a periodic structure. The distance between the unit cell and Floquet port is 15 mm as shown in

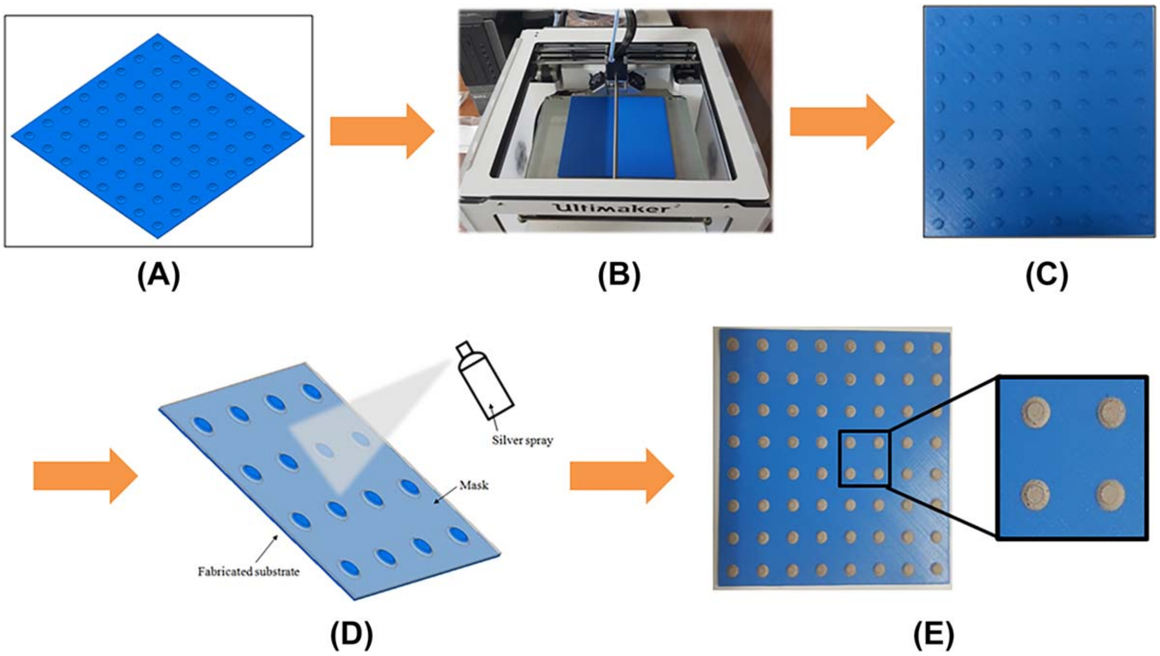

FIGURE 5 Process of fabricating the proposed absorber: A, design; B, 3D printing; C, printed substrate; D, coat silver; and E, the fabricated sample [Color figure can be viewed at wileyonlinelibrary.com]

Figure 2D. Finally, the master/slave boundary conditions are assigned as shown in Figure 2E in order to realize an infinite periodic structure.

The resonant frequency of the metamaterial absorber is affected by the inductance (L) and capacitance (C) as shown below

$$f = \frac{1}{2\pi\sqrt{LC}} \tag{1}$$

The resonant frequency can be reduced by the 3D geometry. The proposed 3D circular truncated cone in Figure 3B is motivated from the 2D circular patch as shown in Figure 3C. We can decrease the footprint size of the unit cell by

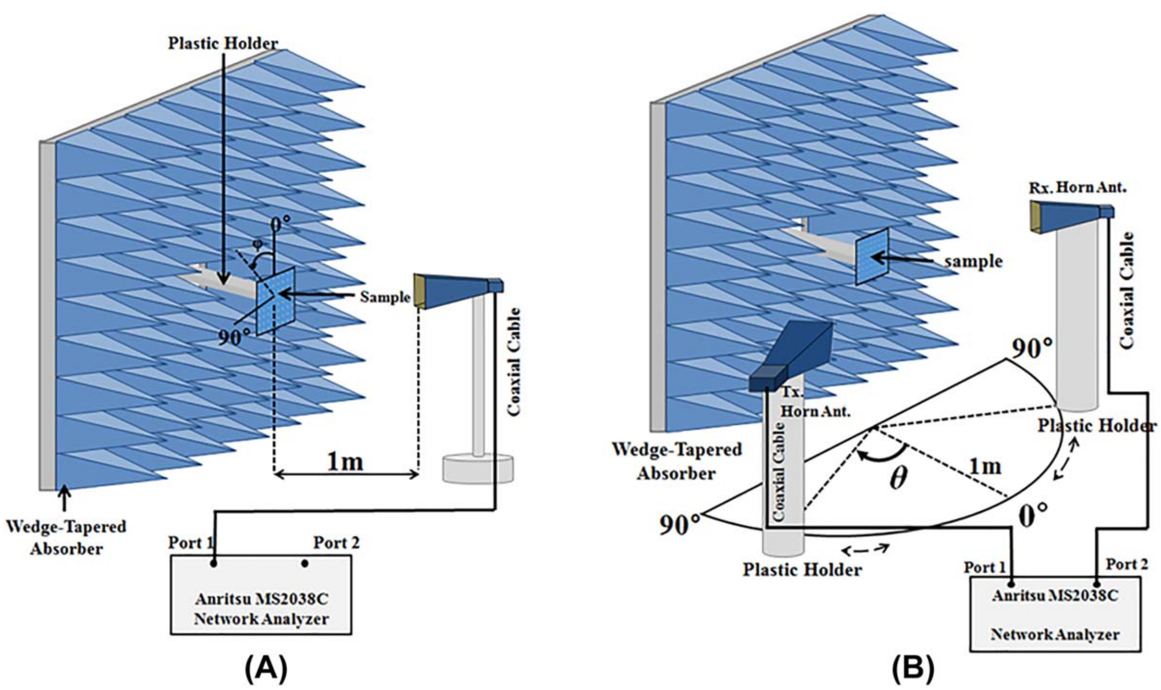

FIGURE 6 Illustration of free-space measurement setup for A, normal incidence and B, oblique incidence [Color figure can be viewed at wileyonlinelibrary.com]

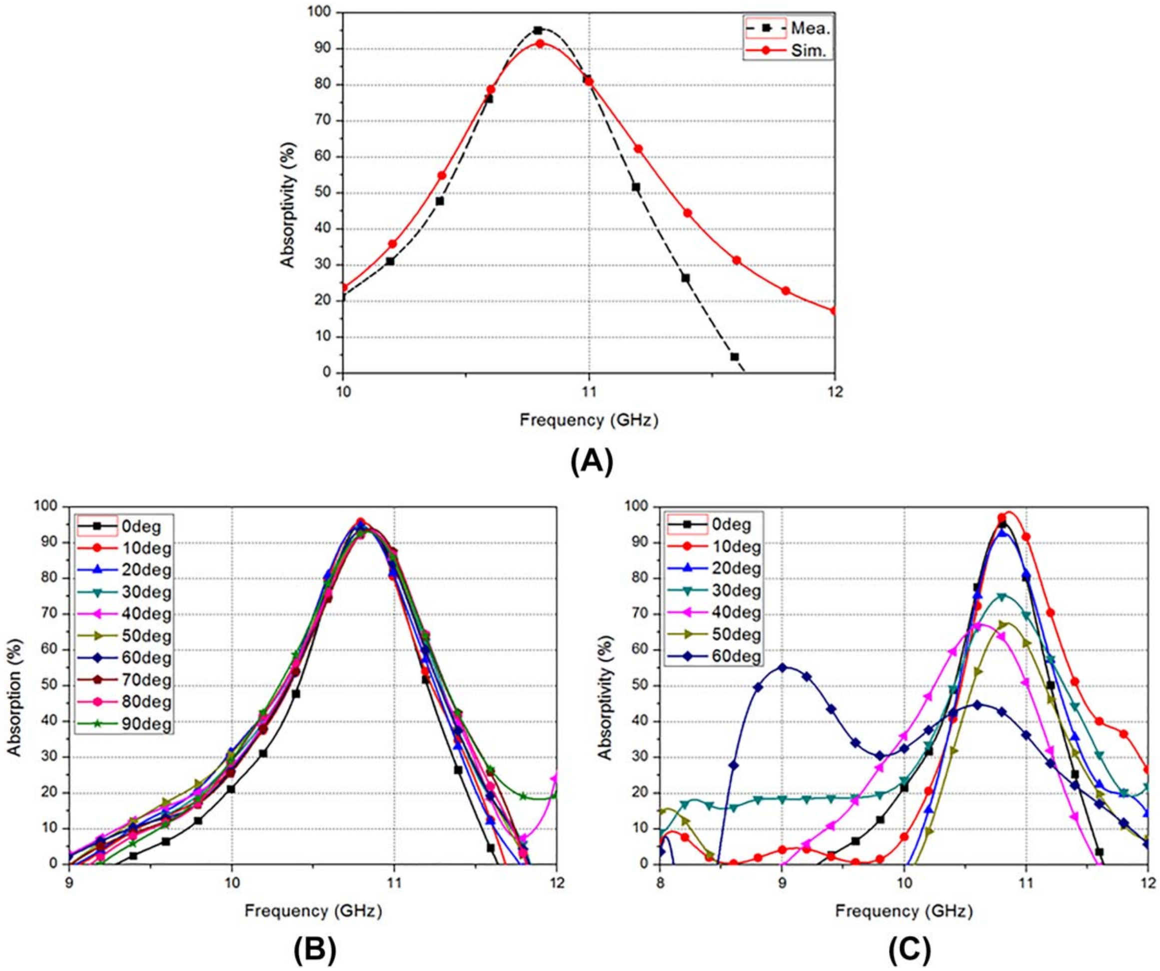

FIGURE 7 A, Simulated and measured absorptivity of the proposed absorber under normal incidence. The measured absorptivity values of the fabricated sample B, for different polarization (φ) values, under normal incidence and C, for different incidence angle (θ) [Color figure can be viewed at wileyonlinelibrary.com]

introducing 3D geometry by increasing effective inductance. It is demonstrated from the simulated S-parameters of the 2D circular patch and 3D circular cone. As shown in Figure 3A, although their diameter on the footprint is same as 8.4 mm, the resonant frequency of the 3D circular cone is 10.81 GHz while that of the 2D circular patch is 12.65 GHz.

Figure 4 shows the simulation results of the proposed absorber for different parameters. In Figure 4A, Di is varied from 3.2 to 6.4 mm with fixed $L = 21$, Do = 8.4, Tp = 11 mm, and Ts = 0.55 mm. It is observed that the resonant frequency is decreased with larger Di because of high inductance. In Figure 4B, Do is varied from 8 to 8.8 mm with fixed $L = 21$, Di = 4.8, Tp = 11 mm, and

TABLE 1 Compared performance of the proposed metamaterial absorber with previously reported metamaterial absorbers using other fabrication process

	Resonant frequency	Fractional bandwidth	Fabrication process	Price
Proposed work	10.81 GHz	2%	3D Printing—silver spray	Low
Ref. [22]	0.8 GHz	4.3%	3D Printing: liquid metal	Medium
Ref. [23]	9.09 GHz	7.2%	Inkjet printing on paper	High
Ref. [24]	10.07 GHz	5%	Optical lithography	High
Ref. [25]	10.44 GHz	4%	Single-layer PCB etching	High
Ref. [26]	10.28 GHz	2%	Multi-layer PCB etching	Very high

Ts = 0.55 mm. It is observed that the resonant frequency is decreased with larger Do because of high inductance. The effect of Do on the resonant frequency is higher than Di. In Figure 4C, Tp is varied from 0.5 to 1.7 mm with fixed $L = 21$, Di = 4.8, Do = 8.4, and Ts = 0.55 mm. It is observed that the resonant frequency is decreased with thicker Tp because of high inductance. In Figure 4D, Ts is varied from 0.35 to 0.75 mm with fixed $L = 21$, Di = 4.8, Do = 8.4, and Tp = 11 mm. As Ts increases, capacitance between the top and bottom plates is decreased. Therefore, the frequency is increased with thicker Ts. The effect of the loss tangent of the PLA dielectric material is investigated. At different loss tangent of 0.007, 0.07, 0.7, and 7, the absorptivity is simulated while fixing $L = 21$, Di = 4.8, Do = 8.4, Tp = 11 mm, and Ts = 0.55 mm. As shown in Figure 4E, when loss tangent is 0.07 and 0.007, the absorptivity is 91% and 58%, respectively. Therefore, the highest absorptivity is observed when the loss tangent is 0.07.

3 | FABRICATION AND RESULTS

Figure 5 shows the fabrication process of the proposed metamaterial absorber sample. First, we designed a model of the substrate using a 3D modeler program, as shown in Figure 5A. We then printed the substrate using a 3D printer (Ultimaker2, Geldermalsen, The Netherlands), as shown in Figure 5B. Figure 5C shows the printed substrate.

The truncated cone is coated by Super Shield™ Silver Coated Copper Conductive Coating (MG Chemicals, Surrey, B.C., Canada), as shown in Figure 5D. To accurately coat the silver spray onto the truncated cone, we used a mask, as shown in Figure 5D. Figure 5E shows the fabricated prototype, with 8 × 8 unit cells. The size of the overall prototype is 168 mm × 168 mm. Copper tape is attached to the bottom plane of the 3D printed substrate.

Figure 6 illustrates the test setup to measure the absorptivity of the proposed absorber. We measured the reflection coefficient with an Anritsu MS2038C vector network analyzer (VNA), wedge-tapered absorber, and 2 horn antennas. The horn antenna was positioned 1 m from the sample in order to satisfy the far field condition. Our measurements indicated that the signal from the horn antenna was reflected from the target. The wedge-tapered absorber was installed on the backside to remove other waves not going to the target

When the sample is measured for different polarization angles (φ) under normal incidence, a single horn antenna is used and the sample is rotated as shown in Figure 6A. In order to measure the absorptivity at different oblique incidence angles (θ), the sample is fixed and the 2 horn antennas are rotated as shown in Figure 6B. The receiving antenna is placed at the specular angle of the transmitting antenna's angle.

The absorptivity can be calculated from the reflection coefficient ($\Gamma(\omega)$) and the transmission coefficient ($T(\omega)$). The absorptivity is calculated as

$$A(\omega) = 1 - \Gamma(\omega) - T(\omega) \tag{2}$$

Because we attached copper tape to the bottom plane of the absorber, the magnitude of transmission coefficient is zero. Therefore, the absorptivity can be calculated from the reflection coefficient alone, by assuming zero transmission. The reflection coefficient of the sample can be determined by subtracting the magnitude of the signal reflected from the sample from the magnitude of the signal reflected from a metal plate (which is of the same size as the sample).

Figure 7A shows the simulated and measured absorptivity values of the proposed absorber under normal incidence. It shows 95% absorptivity at 10.81 GHz from the empirical results, and 91% absorptivity at 10.8 GHz was obtained from the simulation. The fractional bandwidths are 1.11% and 1.94%, from the simulation and measurement results, respectively.

The fractional bandwidth is calculated as

$$\text{Fractional Bandwidth} = \frac{(f_{high} - f_{low})/(f_{high} + f_{low})}{2} \times 100\%, \tag{3}$$

where f_{high} and f_{low} are highest and lowest frequencies when the absorptivity is 90%.

Figure 7B shows the measured results of the sample for different polarization angles under normal incidence. We varied the polarization angle from 0° to 90° at 10° intervals. At each angle, we varied the resonant frequency from 10.74 to 10.84 GHz. Our finding is that the absorptivity is maintained above 90% at all throughout the test. Figure 7C shows the measurement results of the sample for different incidence angles (θ). The absorptivity of the sample is found to be more than 90% for incident angles of up to 20°.

4 | CONCLUSION

In this work, we propose a low-cost three-dimensional (3D) printed metamaterial absorber. The proposed absorber has a circular truncated cone shape to minimize size. The proposed absorber is fabricated by using 3D printing technology; while the silver-coated copper conductive coating spray is used to minimize cost. To test the performance of the proposed absorber, a sample of size 168 mm × 168 mm (8 × 8 unit cells) is fabricated. The measured absorptivity is 91% at 10.81 GHz for normal incidence. In Table 1, we compared the performances and manufacturing cost of the proposed metamaterial absorber with previously reported MM absorbers built in other fabrication technology. The proposed metamaterial absorber has a benefit of low manufacturing cost with acceptable absorptivity. In order to improve the bandwidth of the proposed metamaterial absorber, we will build the 3D printed structure with resistive patterns as a future work.

ACKNOWLEDGMENTS

This research was supported by Chung-Ang University Research Scholarship Grants in 2016 and the Chung-Ang University Graduate Research Scholarship in 2017.

CONFLICTS OF INTEREST

The authors declare no conflicts of interest.

ORCID

Sungjoon Lim http://orcid.org/0000-0002-5049-9300

REFERENCES

[1] Smith DR, Smith DR, Pendry JB, Wiltshire MCK. Metamaterials and negative refractive index. *Science.* 2004;305(5685):788–792. https://doi.org/10.1126/science.1096796

[2] Chen H, Wu BI, Zhang B, Kong JA. Electromagnetic wave interactions with a metamaterial cloak. *Phys Rev Lett.* 2007;99(14):1–4. https://doi.org/10.1103/PhysRevLett.99.063903

[3] Kim DY, Yoon YH, Jo KJ, Jung GB, An CC. Effects of sheet thickness on the electromagnetic wave absorbing characterization of Li 0.375 Ni 0.375 Zn 0.25-ferrite composite as a radiation absorbent Material. *J Electromagn Eng Sci.* 2016;16(3):150–158.

[4] Landy NI, Sajuyigbe S, Mock JJ, Smith DR, Padilla WJ. Perfect metamaterial absorber. *Phys Rev Lett.* 2008;100(20):1–4. https://doi.org/10.1103/PhysRevLett.100.207402

[5] Park MJ, Kim SS. Wide bandwidth pyramidal absorbers of granular ferrite and carbonyl iron powders. *Dig Intermag Conf.* 2000;36: FQ–2. https://doi.org/10.1109/INTMAG.2000.872232

[6] Fante RL, Mccormack MT. Reflection properties of the salisbury screen. *IEEE Trans Antennas Propag.* 1988;36(10):1443–1454. https://doi.org/10.1109/8.8632

[7] Shen X, Cui TJ, Zhao J, Ma HF, Jiang WX, Li H. Polarization-independent wide-angle triple-band metamaterial absorber. *Optical Express.* 2011;19(10):9401–20312.

[8] Lee J, Lee B. Design of thin RC absorbers using a silver nanowire resistive screen. *J Elecromagn Eng Sci.* 2016;16(2):106–111. https://doi.org/10.5515/JKIEES.2016.16.2.106

[9] Kim OS. 3D printing electrically small spherical antennas. In: IEEE Antennas and Propagation Society International Symposium; 2013:776–777. https://doi.org/10.1109/APS.2013.6711047

[10] Lopez AG, Lopez EEC, Chandra R, Johansson AJ. Optimization and fabrication by 3D printing of a volcano smoke antenna for UWB applications. In: 7th European Conference on Antennas Propagation, EuCAP 2013; 2013: 1471–1473.

[11] Carmon TF, Maimon OZ, Dar-El EM. Group set-up for printed circuit board assembly. *Int J Prod Res.* 1989;27(10):1795–1810. https://doi.org/10.1080/00207548908942655

[12] Ahmadloo M, Mousavi P. A novel integrated dielectric-and-conductive ink 3D printing technique for fabrication of microwave devices. In: *IEEE MTT-S International Microwave Symposium Digest*; 2013:1–3. https://doi.org/10.1109/MWSYM.2013.6697669

[13] Sandron S, Heery B, Gupta V, et al. 3D printed metal columns for capillary liquid chromatography. *Analyst.* 2014;139(24):6343–6347., https://doi.org/10.1039/C4AN01476F

[14] Czyżewski J, Burzyński P, Gaweł K, Meisner J. Rapid prototyping of electrically conductive components using 3D printing technology. *J Mater Process Technol.* 2009;209(12–13):5281–5285. https://doi.org/10.1016/j.jmatprotec.2009.03.015

[15] Aguilera E, Ramos J, Espalin D, et al. 3D printing of electro mechanical systems. In: *Proceedings of 24th Annual Solid Freedom Fabrication Symposium*; 2013:950–961. http://www.scopus.com/inward/record.url?eid=2-s2.0-84898415151&partnerID=40&md5=980ee010286f12d903c2e363386cdc9e\nhttp://sffsymposium.engr.utexas.edu/2013TOC.

[16] Chieh JCS, Dick B, Loui S, Rockway JD. Development of a ku-band corrugated conical horn using 3-d print technology. *IEEE Antennas Wireless Propag Lett.* 2014;13:201–204. https://doi.org/10.1109/LAWP.2014.2301169

[17] Yahiaoui R, Guillet JP, de Miollis F, Mounaix P. Ultra-flexible multiband terahertz metamaterial absorber for conformal geometry applications. *Opt Lett.* 2013;38(23):4988–4990. https://doi.org/10.1364/OL.38.004988.

[18] Yahiaoui R, Hanai K, Takano K, et al. Trapping waves with terahertz metamaterial absorber based on isotropic Mie resonators. *Opt Lett.* 2015;40(13):3197, https://doi.org/10.1364/OL.40.003197

[19] Yahiaoui R, Tan S, Cong L, Singh R, Yan F, Zhang W. Multispectral terahertz sensing with highly flexible ultrathin metamaterial absorber. *J Appl Phys.* 2015;118(8):083103 https://doi.org/10.1063/1.4929449

[20] Cong L, Tan S, Yahiaoui R, Yan F, Zhang W, Singh R. Experimental demonstration of ultrasensitive sensing with terahertz metamaterial absorbers: A comparison with the metasurfaces. *Appl Phys Lett.* 2015;106(3):031107 https://doi.org/10.1063/1.4906109

[21] Lee D, Hwang JG, Lim D, Hara T, Lim S. Incident angle- and polarization-insensitive metamaterial absorber using circular sectors. *Sci Rep.* 2016;6(1):27155 https://doi.org/10.1038/srep27155

[22] Kim HK, Lee D, Lim S. Wideband-switchable metamaterial absorber using injected liquid metal. *Sci Rep.* 2016;6(1):31823 https://doi.org/10.1038/srep31823

[23] Yoo M, Kim HK, Kim S, Tentzeris M, Lim S. Silver nanoparticle-based inkjet-printed metamaterial absorber on flexible paper. *IEEE Antennas Wireless Propag Lett.* 2015;14:1718–1721. https://doi.org/10.1109/LAWP.2015.2420712

[24] Cheng Y, Yang H, Cheng Z, Xiao B. A planar polarization-insensitive metamaterial absorber. *Photon Nanostruct Fundam. Appl.* 2011;9(1):8–14. https://doi.org/10.1016/j.photonics.2010.07.002

[25] Zhu B, Wang Z, Huang C, Feng Y, Zhao J, Jiang T. Polarization insensitive metamaterial absorber with wide incident angle. *Prog Electromagn Res.* 2010;101:231–239. https://doi.org/10.2528/PIER10011110

[26] Yoo M, Kim HK, Lim S. Angular-and polarization-insensitive metamaterial absorber using subwavelength unit cell in multi-layer technology. *IEEE Antennas and Wireless Propagation Letters.* 2016;15:414–417.

How to cite this article: Yoon Y, Lim D, Tentzeris MM, Lim S. Low-cost metamaterial absorber using three-dimensional circular truncated cone. *Microw Opt Technol Lett.* 2018;60:1622–1630. https://doi.org/10.1002/mop.31211

Received: 28 November 2017

DOI: 10.1002/mop.31210

Antenna sensitivity enhancement using ground shorting pin

Hongkoo Lee | **Longyue Qu** | **Hyeongdong Kim**

Department of Electronics and Communications Engineering, Hanyang University, Haengdang-dong, Seongdong-gu, Seoul, Korea

Correspondence
Hyeongdong Kim, Department of Electronics and Communications Engineering, Hanyang University, Haengdang-dong, Seongdong-gu, Seoul, Korea.
Email: hdkim@hanyang.ac.kr

Funding information
Institute for Information & Communications Technology Promotion (IITP) of Korea Government (MSIT), Grant/Award Number: 2013-0-00401

Abstract

This article proposes a design technique to increase the sensitivity of Bluetooth headset antennas. A planar inverted F antenna was designed on the top printed circuit board (PCB) of a two-board PCB. Digital noise was designed as a loop-type source on the bottom PCB, representing general noise derived from digital circuits and digital noise generated from the main cable line. The proposed antenna design was analyzed by means of simulation and verified by means of measurements of a fabricated antenna. The proposed technique increased the measured sensitivity by 2.23 dB.

KEYWORDS

digital noise, ground shorting pin, planar inverted-F antenna, total isotropic sensitivity, total radiated power

1 | INTRODUCTION

With the advent of Bluetooth services, wireless headsets have become more common. However, designing a highly sensitive antenna in a small Bluetooth headset is a great challenge for antenna designers. The performance of a receiving antenna is affected by bit error rate and signal-to-noise ratio. Noise performance is an important factor affecting the minimum signal level the receiving antenna can recognize.[1–3] In a wireless communication system, the noise source that affect the antenna performance are usually man-made, arising from high-speed digital circuits. In an active measurement, total isotropic sensitivity (TIS) is affected by the antenna efficiency, noise interference, and conductive sensitivity.[1] To increase the sensitivity of the receiving antenna, either the efficiency of the antenna has to be increased or the interference of the noise has to be reduced.

Many studies have focused on the use of parasitic slots and characteristic modes for decoupling in a multi-input and multi-output (MIMO) systems[4–6] and increasing TIS on a single board.[7,8] In this letter, the concept of decoupling digital noise from the antenna is discussed. As an example, modeling of a two board Bluetooth headset was conducted based on commercial board. Simulation was conducted using full wave simulator and measurement data were verified using active measurements of Bluetooth headsets in a 6 m × 3 m × 3 m three-dimensional (3-D) Cellular Telecommunications and Internet Association over the air (CTIA OTA) chamber using a TC-3000B Bluetooth tester.

2 | ANTENNA DESIGN AND OPERATING MECHANISM

As shown in Figure 1, the proposed PIFA (10 mm × 5 mm) was designed on the top PCB (10.5 mm × 19.5 mm) ground plane of a Bluetooth headset. This PIFA had the form of a bended radiator to be made applicable to an actual commercial board. The top PCB was connected to the bottom PCB through a signal connector. The signal connector is usually a complicated board-to-board connector as shown in Figure 4, but for simulation the signal connector was simplified to a line connecting top and bottom PCB. For simulation, a loop-type resonator was formed on the bottom PCB (10.5 mm × 15 mm) to represent digital noise. The digital noise occurring on commercial boards is mostly undefinable, but takes a form of a loop. Therefore, for simulation, it was simplified and designed as a loop type resonator on the bottom PCB.[7,8] Digital noise is coupled to the antenna through the signal connector, thereby degrading the antenna sensitivity. Thus, to reduce the coupling between the digital noise and the antenna, an additional ground shorting pin was designed to distribute the current path.